chemosensors

MDPI

Article

Model Development for Alcohol Concentration in Exhaled Air at Low Temperature Using Electronic Nose

Lidong Tan [1], Jiexi Wang [1], Guiyou Liang [2,*], Zongwei Yao [3], Xiaohui Weng [3], Fangrong Wang [4] and Zhiyong Chang [5,6,*]

1 College of Transportation, Jilin University, Changchun 130022, China
2 Research and Development Institute, China FAW Group Co., Ltd., Changchun 130013, China
3 School of Mechanical and Aerospace Engineering, Jilin University, Changchun 130022, China
4 College of Communication Engineering, Jilin University, Changchun 130012, China
5 Key Laboratory of Bionic Engineering, Ministry of Education, Jilin University, Changchun 130022, China
6 College of Biological and Agricultural Engineering, Jilin University, Changchun 130022, China
* Correspondence: liangguiyou@faw.com.cn (G.L.); zychang@jlu.edu.cn (Z.C.)

Abstract: Driving safety issues, such as drunk driving, have drawn a lot of attention since the advent of shared automobiles. We used an electronic nose (EN) detection device as an onboard system for shared automobiles to identify drunk driving. The sensors in the EN, however, can stray in cold winter temperatures. We suggested an independent component analysis (ICA) correction model to handle the data collected from the EN in order to lessen the impact of low temperature on the device. Additionally, it was contrasted with both the mixed temperature correction model and the single temperature model. As samples, alcohol mixed with concentrations of 0.1 mg/L and 0.5 mg/L were tested at (20 ± 2) °C, (−10 ± 2) °C, and (−20 ± 2) °C. The results showed that the ICA correction model outperformed the other models with an accuracy of 1, precision of 1, recall of 1, and specificity of 1. As a result, this model can be utilized to lessen the impact of low temperature on the EN's ability to detect the presence of alcohol in the driver's inhaled gas, strongly supporting its use in car-sharing drink driving. Other ENs that need to function in frigid conditions can also use this technique.

Keywords: electronic nose; low temperature; temperature correction; independent component analysis; support vector machine; drink driving detection

Citation: Tan, L.; Wang, J.; Liang, G.; Yao, Z.; Weng, X.; Wang, F.; Chang, Z. Model Development for Alcohol Concentration in Exhaled Air at Low Temperature Using Electronic Nose. *Chemosensors* **2022**, *10*, 375. https://doi.org/10.3390/chemosensors10090375

Academic Editor: Antonio Pardo Martínez

Received: 19 August 2022
Accepted: 14 September 2022
Published: 19 September 2022

1. Introduction

The development of vehicle sharing in recent years has made daily travel easier for people. However, as the car-sharing sector has grown, preventing drivers from operating shared vehicles while intoxicated has become a critical issue [1]. The majority of the time, law enforcement personnel test drivers with handheld alcohol detectors by observing how they are operating their vehicles. However, manual detection to check on drivers' levels of intoxication needs a significant amount of manpower, which wastes resources, has low detection efficiency and a limited range [2] and is easily influenced by other factors [3]. Gas chromatographs [4], gas chromatograph-mass spectrometers [5], and other instruments have been frequently used in the past to measure gas composition, but the majority of them are pricey and have lengthy detection times, making them unsuitable for determining whether or not drivers have consumed alcohol.

Lightweight and non-contact electronic noses (EN) are of interest to address the aforementioned issues. The EN primarily consists of three functional components, namely an odor sampling operator, a gas sensor array, and a signal processing system [6]. These components work together to swiftly offer an overview of the sample that was detected using specialized sensors and recognition modules. The EN is well suited for odor detection in confined places, including space stations [7,8], space shuttles [9,10], and vehicles [11].

However, the EN might drift due to temperature, and other factors, including humidity [12] and aging components [13], which is a worry. The gas sensor is the main component of the EN, and the metal oxide type sensor is the most used. The metal oxide sensor's working theory is that, at a given temperature, the chemical interaction between the measured gas reaching the semiconductor surface and the oxygen adsorbed on the semiconductor surface is accompanied by charge transfer, which further causes the semiconductor's resistance to change. The detection of gas is accomplished by detecting the change in semiconductor resistance. We know that a semiconductor's resistance varies with temperature in a nonlinear manner from the theory of semiconductors. This means that, within a given temperature range, the resistance of the gas sensor increases when the environment becomes cold and reduces when the ambient temperature rises [14–16]. In order for metal oxide sensors to function properly, this establishes the requirement for optimal temperature conditions.

It has been challenging to identify and discard sensor drift caused by temperature fluctuations brought on by changes in the environment. The accuracy of the model will be impacted if the drift in the sensor signal is not adjusted [17]. The effect of temperature interference on the gas sensor is considerably more pronounced when the sensor is mounted to the e-nose, and the temperature of the sample and the environment in which it is placed may result in the incorrect categorization of the EN [18]. Winter temperatures may drop to tens of degrees below zero in numerous places across the world, including northeast China, where they can fall below −20 °C. The impact of temperature becomes more evident if we wish to assure reliable detection of alcohol gas content in the driver's exhaled breath when there are specific weather circumstances.

Heating or cooling the sensor and temperature compensation using algorithms are two correction techniques to lessen the impact of temperature on the sensor. Jian-Wei Gong et al. added a temperature control module to the gas sensor circuit to assure the proper temperature [14,19]; however, this caused the circuit to heat up unevenly. The influence of temperature disturbances on the mems gyroscope was reduced by Youqi Jiang et al. using a semiconductor TEC thermostat and a PID control algorithm optimized using an ant colony algorithm [20]. However, this technique requires more preparation time. Due to its low cost and excellent accuracy, software methods are frequently utilized in the sensor temperature compensation problem [21]. To create a model for precise temperature compensation, Xin Yu et al. collected two typical characteristics of methane detecting equipment and their connection with temperature [22]. By adjusting the curve of temperature and pressure sensor resistance to the temperature compensation model, Liu Xun et al. created a temperature compensation model [23]. Such models, however, are constrained and only relevant to particular sensors. In order to lessen the impact of temperature on the sensor, mathematical techniques, such as temperature gradient field compensation [24], real-time temperature compensation models [25,26], higher-order Fourier transforms [27], random forests [28], and neural networks [29–32], are frequently used. These techniques have produced generally positive results and increased sensor accuracy. Their disadvantage is that they necessitate a lot of experimentation and make model construction more challenging. Researchers have also developed mathematical models for e-nose drift compensation, but all of them are difficult to use in EN under low-temperature conditions [33–35]. The EN may become more popular if a model is researched and applied to it so that it may work in low-temperature conditions without having the aforementioned issues and effectively weaken the effect of temperature.

The goal of this study was to reduce the mixed gas alcohol concentration low-temperature effect for in-vehicle EN identification using a correction model created using an independent component analysis (ICA) calibration model with a support vector machine (SVM) to distinguish driver intoxication while operating a vehicle. By contrasting the single temperature model and the mixed temperature calibration model, the optimal model to minimize temperature drift was found.

2. Materials and Methods

2.1. Samples

Driving after drinking is defined as behavior while operating a vehicle with a blood alcohol content greater than or equal to 20 mg/100 mL and less than 80 mg/100 mL, according to standards set forth by China's State Administration of Quality Supervision, Inspection, and Quarantine. Driving while intoxicated is defined as having a blood alcohol concentration of at least 80 mg/100 mL. The threshold for driving after drinking is an exhaled gas alcohol concentration larger than or equal to 0.09 mg/L and less than 0.36 mg/L, as calculated by the formula (1) from the relationship between blood alcohol concentration (*BAC*) and breathed gas alcohol concentration (*BrAC*) (Table 1). The legal limit for drunk driving is 0.36 mg/L of alcohol or more in the driver's exhaled gas:

$$BAC = BrAC \times 2200 \quad (1)$$

Table 1. Standard alcohol content for driving after drinking and drunk driving.

Behavior Category	Blood Alcohol Content (*BAC*) mg/100 mL	Breath Alcohol Content (*BrAC*) mg/L
Driving after drinking	>20 and <80	>0.09 and <0.36
Drunk driving	>80	>0.36

The exhaled gases from the simulated drivers who had consumed alcohol while driving had an alcohol concentration of 0.1 mg/L, 5% carbon dioxide, 16% oxygen, and the remainder was nitrogen. The gases were set up to replicate various driving circumstances after drinking [36]. The exhaled gas of the drunk driver had a simulated alcohol concentration of 0.5 mg/L and was composed primarily of nitrogen, with just 5% of carbon dioxide and 16% oxygen. Changchun Juyang Gas Co., Ltd. configured the gas, and following configuration, the gas was transferred to the laboratory.

2.2. Electronic Nose Detection System

The EN system (Figure 1a) employed in this work was created internally and consisted of an air pump, a bionic detecting chamber [37,38], a gas sensor array, a signal conditioning circuit, a data collector, a computer, etc. In Figure 1b, the hardware composition is displayed. Due to the fact that human exhalation is a mixture of gases, the sensor array used 32 metal oxide sensors, each of which had the details listed in Table 2. They work at an ambient temperature limited to near −10 °C to 50 °C, and the optimal operating ambient temperature is about 20 °C. Moreover, the sensor cannot operate near the limited temperature for a long time. The data were recorded using the acquisition software that was included with the data acquisition equipment after the resistance signal produced by the sensors was converted into a voltage signal by a signal conditioning circuit and sent to the computer.

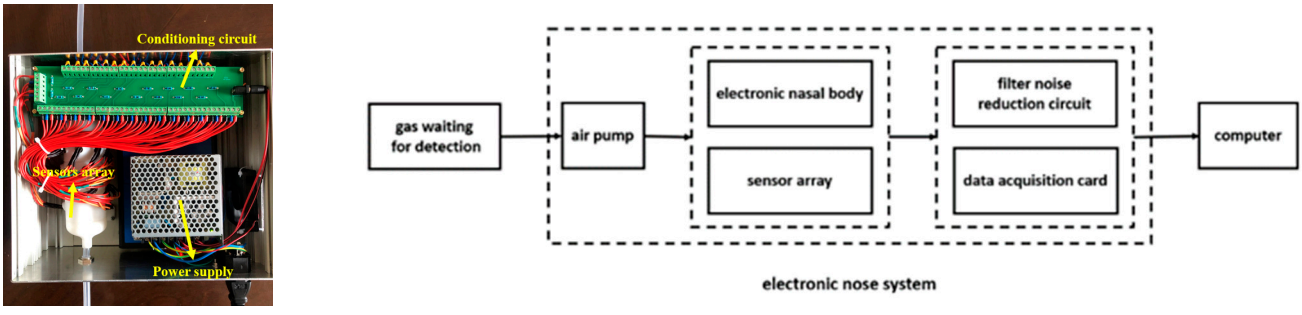

(**a**) (**b**)

Figure 1. (**a**) EN physical diagram; (**b**) Schematic diagram of the EN structure.

Table 2. Sensors in the sensor array.

Sensor	Target Gases	Maker
TGS2612	methane, propane, butane	Figaro
TGS2611	methane	Figaro
TGS2620	alcohol	Figaro
TGS2603	VOC	Figaro
TGS2602	VOC	Figaro
TGS2610	propane, butane	Figaro
TGS2600	cigarette smoke	Figaro
GSBT11	VOC	Ogam
MS1100	formaldehyde, VOC	Ogam
MP135	hydrogen, alcohol, carbon monoxide	Winson
MP901	alcohol, smoke, formaldehyde, toluene, benzene, acetone	Winson
MP-9	carbon monoxide, methane	Winson
MP-3B	alcohol	Winson
MP-4	methane, natural gas, biogas	Winson
MP-5	propane	Winson
MP-2	propane, smoke	Winson
MP503	alcohol, smoke, isobutane, formaldehyde	Winson
MP801	benzene, toluene, formaldehyde, alcohol, smoke	Winson
MP905	benzene, toluene, formaldehyde, alcohol, smoke	Winson
MP402	methane, propane	Winson
WSP1110	nitrogen dioxide	Winson
WSP2110	toluene, formaldehyde, benzene, alcohol, acetone	Winson
WSP7110	hydrogen sulfide	Winson
MP-7	carbon monoxide	Winson
TGS2612	methane, propane, butane	Figaro
TGS2611	methane	Figaro
TGS2620	alcohol	Figaro
MP-3B	alcohol	Winson
MP702	ammonia	Winson
TGS2610	propane, butane	Figaro
TGS2600	cigarette smoke	Figaro
TGS2618-COO	butane, liquified petroleum (gas)	Figaro

2.3. Data Collection and Pretreatment

Northeastern China's distinct geographic location causes the wintertime outdoor temperature to drop as low as −20 °C. For a certain amount of time, the temperature inside a stationary car will be lower than the outside temperature. To imitate a lower temperature, this experiment was carried out in the open air. A temperature sensor was used to gauge the outside temperature. The EN was turned on while standing for 20 min, causing the temperature of two gas mixes with various alcohol concentrations to drop to the outdoor temperature as soon as the temperature approached the target range. Then, data on gas composition were gathered using the EN. The sample was put close to the EN's inlet, and a rubber hose was used to deliver gas into the device. The responses of 32 sensors in the e-nose sensor array were recorded while the single acquisition time of the e-nose was set to 60 s and the sampling frequency was 100 Hz. The same process was repeated with forty sets of measurements taking place for each concentration sample at the same temperature, with the gas mixture of two concentrations being placed at a room temperature of (20 ± 2) °C, (−10 ± 2) °C, and (−20 ± 2) °C, in turn. The humidity level during the experiment was basically constant and the average humidity was 61.9%, which is a more suitable humidity level.

A total of 32 sensors were tested at various temperatures, yielding a total of 240 sets of data. The baseline response of the alcohol gas-sensitive sensors was found to be moderate and steady in the first stage; in the second stage, the response signal initially displayed an increasing trend before continuing to level out after reaching the maximum value.

The raw data were standardized using z-score to remove the dissimilar dimensions between various indicators, guarantee the quality of the data, and ensure the dependability of the results (standard deviation standardization). The acquired standard data were

distributed normally, with a mean of 0 and a standard deviation of 1 [39]. The equation (2) was used to calculate the z-score standardization:

$$y_i = \frac{x_i - \mu_x}{\sigma_x} \quad (2)$$

where, x_i is the i rd element of the original vector (input or target). μ_x is the mean value of the original vector. σ_x is the standard deviation of the original vector. y_i is the i rd element of the generated vector data.

2.4. Single Temperature Model

Support vector machine (SVM) is a brand-new classification method built on statistical learning that has the benefits of little training data, quick processing, and high accuracy [40]. Based on these benefits, SVM was selected as the model's classifier, and a single temperature prediction model was created using the experimentally obtained data. In this work, all radial basis functions were used as the SVM's kernel function, and a grid-seeking approach was applied to maximize the regularization constants C and γ. The training for set testing the prediction outcomes under various temperature samples were chosen to be the data at (20 ± 2) °C temperature. To categorize the alcohol concentration in the gas, the data at (-10 ± 2) °C and (-20 ± 2) °C temperatures were utilized as the test set.

2.5. Mixed Temperature Correction Model

SVM was used as a classifier to create a mixing temperature adjustment model using data from alcohol gas mixtures at temperatures of 0.1 mg/L and 0.5 mg/L at (20 ± 2) °C and (-20 ± 2) °C, respectively. The model's capacity to categorize various alcohol percentages of gas mixtures at various temperatures was put to the test. The data of (20 ± 2) °C and (-20 ± 2) °C were used as the training set, (20 ± 2) °C, (-10 ± 2) °C, and (-20 ± 2) °C were used as the test set, while the ratio of (20 ± 2) °C and (-20 ± 2) °C in the training and test sets was 7:3.

We chose the data under the temperature conditions of (20 ± 2) °C, (-10 ± 2) °C, and (-20 ± 2) °C and constructed the model in accordance with the above procedure to develop another mixed temperature correction model, where the ratio of the training set and test set was 7:3. We compared the two mixture temperature correction models' abilities to reduce the impact of temperature on the sensor based on the test results.

2.6. ICA Correction Model

Figure 2 illustrates how Independent Component Analysis (ICA), an efficient blind source separation technique, divides the data into linear combinations of statistically distinct non-Gaussian sources [41].

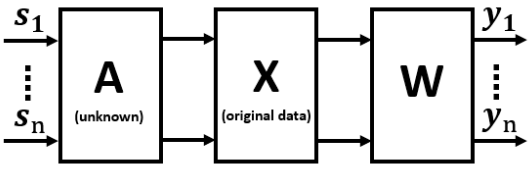

Figure 2. ICA model.

Suppose there are n independent source signals $s_1(t), s_2(t), ..., s_n(t)$, each with discrete form $s_1, s_2, ..., s_n$. $x_1, x_2, ..., x_m$ is the observed m parameters. The purpose of ICA is to estimate the n independent sources from the m detected parameters. The universal ICA model can be written as:

$$X = AS \quad (3)$$

where $X = (x_1, x_2, ..., x_m)^T$ and $x_1, x_2, ..., x_m$, respectively, represent the response of EN to mixed gases with different alcohol concentrations at different temperatures. $S =$

$(s_1, s_2, ..., s_n)^T$. A is a mixed matrix and $A = (a_{ij})$, $1 \leq i \leq m$, $1 \leq j \leq n$. The only prior information is that each component of S is statistically independent. When both S and A are unknown, the goal of ICA is to solve a demixing matrix W and to find the best estimate Y of S by calculating so that the independence between its components is maximized:.

$$Y = WX \tag{4}$$

Because it offers the advantages of quick convergence and may be used to compute any non-Gaussian signal, the Fast ICA technique is employed in this research. It is a negative entropy-based ICA fixed point method. It incorporates negative entropy as an approximation goal function and, through iterative search, discovers the greatest non-Gaussian feature of WX.

First, similar to the procedure in Section 2.3, the data with various alcohol concentrations at (20 ± 2) °C, (−10 ± 2) °C, and (−20 ± 2) °C were preprocessed. The data were then integrated into the ICA model to eliminate the output components of the ICA that were strongly associated with the interference caused by ambient temperature and found the ICA output components that were more strongly correlated with the actual odor signal. Finally, an SVM with a 7:3 training set to test set ratio was used to train and classify the chosen ICA components.

3. Results and Discussion

3.1. Results of the Single Temperature Model

The accuracy of the training set was 1, the precision was 1, the recall was 1, and the specificity was 1, according to the SVM model constructed at (20 ± 2) °C. The test set had an accuracy of 0.8438, a precision of 0.7619, a recall of 1, and a specificity of 0.6875. Figure 3 displays the sensor's response curves at various temperatures. It can be observed that, within a particular temperature range, the sensor reaction steadily shrinks as the temperature drops; 20 °C is the ideal temperature for the sensor to function; the sensor response is most pronounced at this temperature condition. At the same time, the sensor response is more obvious the higher the gas mixture's alcohol concentration, and as the temperature drops, the difference between the sensor response to different gas mixtures' alcohol concentrations gradually narrows. This is because the EN sensor's response includes not only information about odor but also information about temperature, so the temperature has some bearing on the EN. Low temperatures will affect the model's categorization because of the mixed gas's worsening recognition effect.

3.2. Results of Mixed Temperature Correction Model

The training set for the model constructed from data collected at (−20 ± 2) °C and (20 ± 2) °C had an accuracy of 0.9911, a precision of 0.9818, a recall of 1, and a specificity of 0.9828. The test set had an accuracy of 0.9375, a precision of 0.8919, a recall of 1, and a specificity of 0.8710. In the model training set created from data collected at (−20 ± 2) °C, (−10 ± 2) °C, and (20 ± 2) °C, the accuracy was 0.9821, the precision was 0.9651, the recall was 1, and the specificity was 0.9647. The test set's accuracy was 0.9861, precision was 0.9737, recall was 1, and specificity was 0.9714. The mixed temperature adjustment approach, as could be observed, lessens the impact of temperature on the EN's sensors. The choice of more experimental data at multiple temperature settings for model training enhanced the amount of data and allowed the model to produce better results since the results of the model constructed using data at (−20 ± 2) °C, (−10 ± 2) °C, and (20 ± 2) °C were superior to those built using data at (−20 ± 2) °C and (20 ± 2) °C. The mixed temperature correction model lowered the EN's recognition error at various temperatures for various concentrations of alcohol gas mixes as compared to the single temperature model. The samples included in this interval had superior categorization results because the model was based on sensor data collected at various temperatures.

3.3. Results of the ICA Correction Model

After ICA processing, the SVM model's training set had an accuracy of 1, precision of 1, recall of 1, and specificity of 1. The test set had a precision of 1, recall of 1, specificity of 1, and accuracy of 1. The outcomes demonstrate that the ICA algorithm calculation in the preprocessing of the EN information removes the information strongly related to the temperature interference, reduces the data dimension, and maximizes the compensation of the low temperature on the effect brought about by the EN. The ICA correction model greatly lowers the classification error for various concentrations of mixed temperatures when compared to the single-temperature model, demonstrating the superiority of the ICA correction model effect. This model minimizes modeling complexity, sample size eliminates redundant interference information and offers a novel approach for the EN to recognize gases at low temperatures.

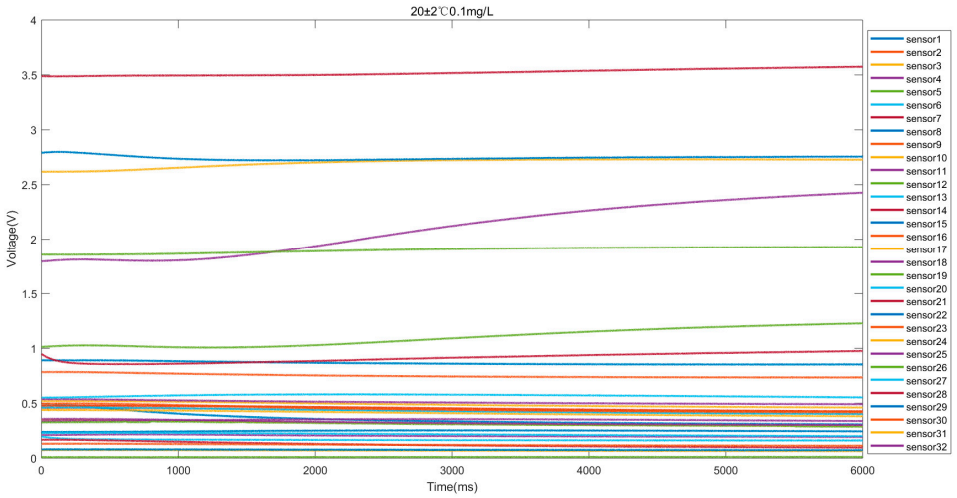

(**a**)

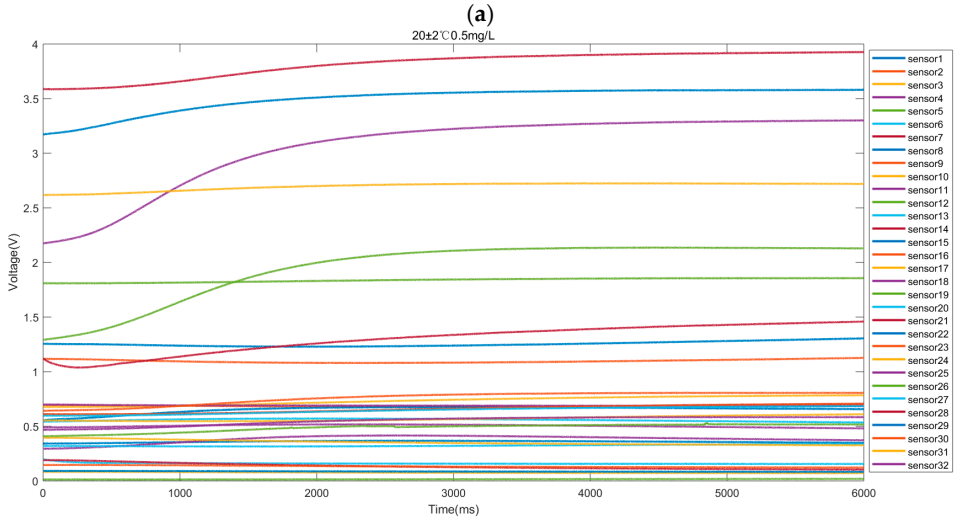

(**b**)

Figure 3. *Cont.*

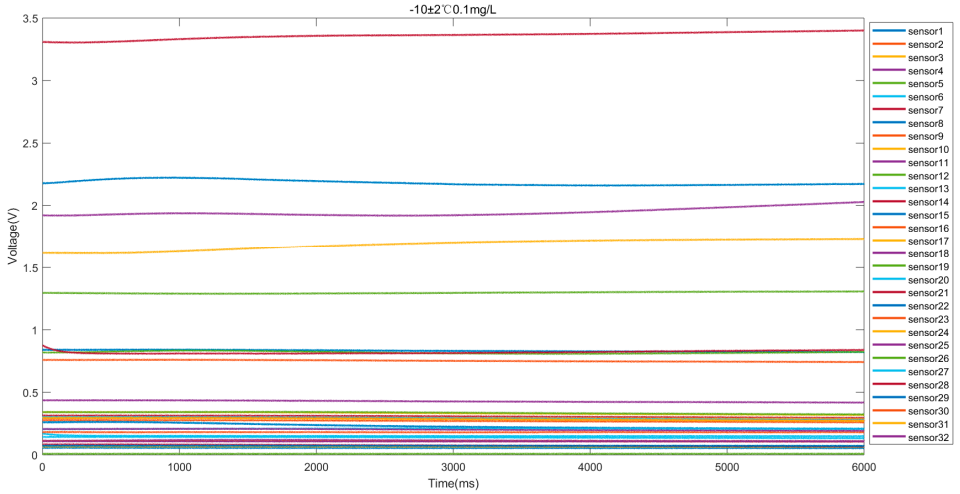

(**c**)

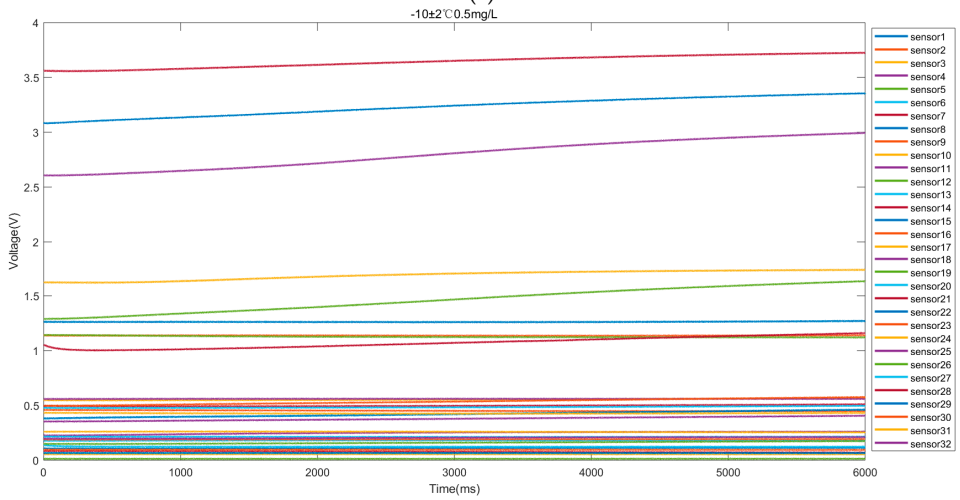

(**d**)

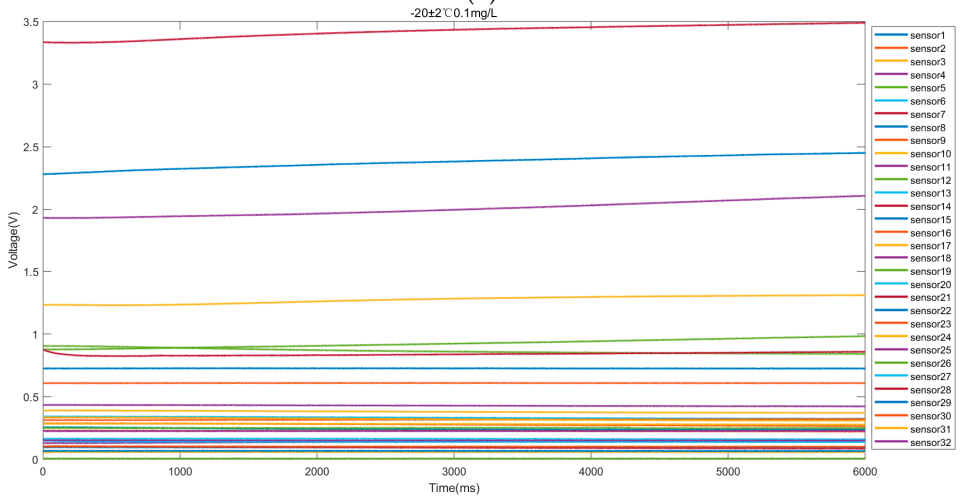

(**e**)

Figure 3. *Cont.*

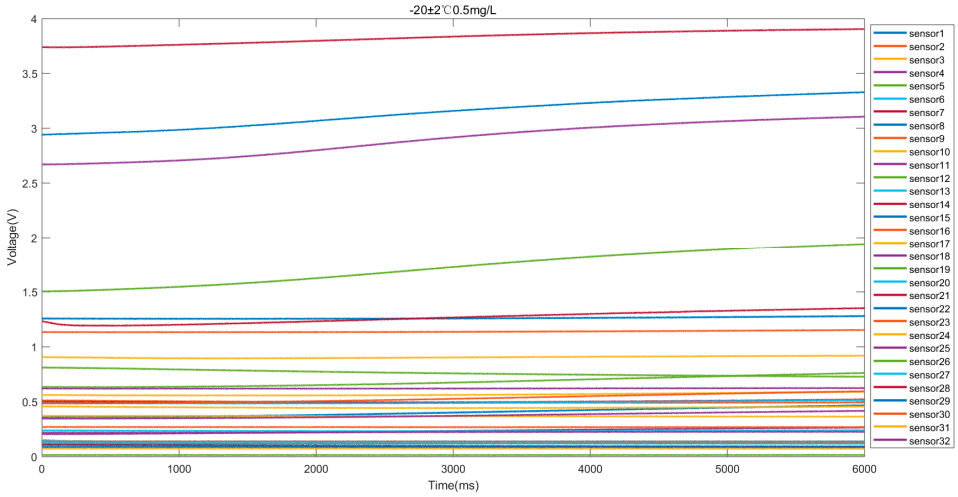

(**f**)

Figure 3. (**a**) (20 ± 2) °C 0.1mg/L sensor response; (**b**) (20 ± 2) °C 0.5 mg/L sensor response; (**c**) (−10 ± 2) °C 0.1 mg/L sensor response; (**d**) (−10 ± 2) °C 0.5 mg/L sensor response; (**e**) (−20 ± 2) °C 0.1 mg/L sensor response; (**f**) (−20 ± 2) °C 0.5 mg/L sensor response.

3.4. Comparison of Model Prediction Results

A single temperature model, two mixed temperature correction models, an ICA correction model, and a fourth model—a total of four models—were created using SVM as a classifier. Figure 4 depicts the confusion matrix of the various models, and Table 3 lists the outcomes. The results of the model show that the EN was impacted by the low temperature. Because these two models incorporated data from various temperature situations and produced superior classification results for the samples in this temperature range, they had better results than the single temperature model. The single temperature model and the two mixed temperature correction models performed worse in terms of processed results than the ICA correction model. Additionally, the single temperature model and the two mixed temperature correction models would need very large samples and quantities in order to produce the same results as the ICA correction model. The effect of low temperature on the EN's ability to detect various quantities of alcohol gas can be successfully mitigated by the ICA correction model.

Table 3. Results of four models.

Model	Type	Accuracy	Precision	Recall	Specificity
Single temperature model	training set	1	1	1	1
	test set	0.8438	0.7619	1	0.6875
Mixed temperature correction model ((−20 ± 2) °C and (20 ± 2) °C)	training set	0.9911	0.9818	1	0.9828
	test set	0.9375	0.8919	1	0.8710
Mixed temperature correction model ((−20 ± 2) °C, (−10 ± 2) °C, and (20 ± 2) °C)	training set	0.9821	0.9651	1	0.9647
	test set	0.9861	0.9737	1	0.9714
ICA correction model	training set	1	1	1	1
	test set	1	1	1	1

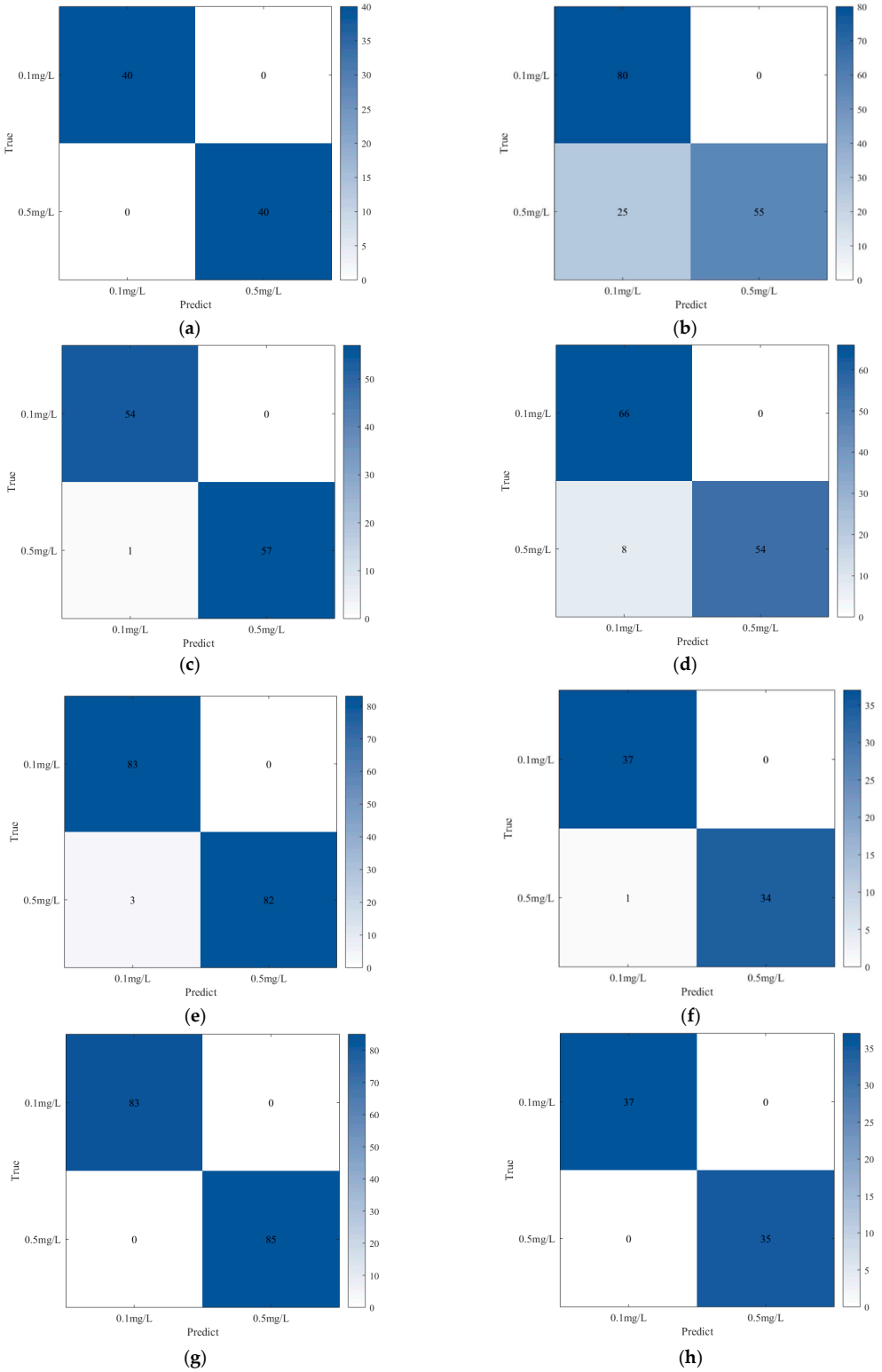

Figure 4. (**a**) Single temperature model training set confusion matrix; (**b**) single temperature model test set confusion matrix; (**c**) (−20 ± 2) °C and (20 ± 2) °C mixed temperature correction model training set confusion matrix; (**d**) (−20 ± 2) °C and (20 ± 2) °C mixed temperature correction model test set confusion matrix; (**e**) (−20 ± 2) °C, (−10 ± 2) °C, and (20 ± 2) °C mixed temperature correction model training set confusion matrix; (**f**) (−20 ± 2) °C, (−10 ± 2) °C, and (20 ± 2) °C mixed temperature correction model test set confusion matrix; (**g**) ICA correction model training set confusion matrix; (**h**) ICA correction model test set confusion matrix.

4. Conclusions

The EN is a metal oxide semiconductor gas sensor system that uses pattern recognition algorithms that are cross-sensitive, selectable, and reliable to various odors [42]. In order to identify the amount of alcohol in the driver's breath, we suggest an in-vehicle lightweight EN for shared vehicles that operate well at low temperatures. First, the signal acquisition hardware was designed, followed by the processing and selection of the sensor array and conditioning circuit for the EN in-vehicle drunk driving detection system. The drift of the metal oxide sensor in the EN in low-temperature conditions was then reduced using four data processing methods. To lessen the impact of low temperature on the system, support vector machines were used as classifiers to create a single temperature model, a mixed temperature correction model, and an ICA correction model. The ICA correction model, which has an accuracy of 1, precision of 1, recall of 1, and specificity of 1, outperforms the other models in terms of recognition rate. The ICA correction model, which does not use a large amount of data for training, performed better than the other models. The EN can be used in long-term low-temperature circumstances with the model suggested in this research, which can lessen the impact of low temperatures on the electronic nose. Additionally, this makes the EN-based in-vehicle drunk driving detection system a potential device for detecting alcohol gas combinations in closed compartments that can continue to function in cold environments. Other EN systems that require low-temperature operation can use this technique as well.

Author Contributions: Conceptualization, L.T., Z.C. and J.W.; investigation, G.L. and X.W.; methodology, validation, formal analysis, data curation, writing—original draft preparation and writing—review and editing, J.W.; supervision, project administration, funding acquisition and writing—review and editing, L.T., X.W., G.L., Z.Y., F.W. and Z.C. All authors have read and agreed to the published version of the manuscript.

Funding: This work was supported by the National Natural Science Foundation of China (51875245), the Science-Technology Development Plan Project of Jilin Province (20200501013GX, 20200403059SF, 20200403064SF), the Special Project of Industrial Technology Research and Development of Jilin Province (2019C039-5, 2020C023-6), the "13th Five-Year Plan" Scientific Research Foundation of the Education Department of Jilin Province (JJKH20211116KJ, JJKH20221018KJ).

Institutional Review Board Statement: Not applicable.

Informed Consent Statement: Not applicable.

Data Availability Statement: The data presented in this study are available on request from the corresponding author.

Conflicts of Interest: The authors declare no conflict of interest.

References

1. Rosero-Montalvo, P.D.; López-Batista, V.F.; Peluffo-Ordóñez, D.H. Hybrid embedded-systems-based approach to in-driver drunk status detection using image processing and sensor networks. *IEEE Sens. J.* **2020**, *21*, 15729–15740. [CrossRef]
2. Zuba, D. Accuracy and reliability of breath alcohol testing by handheld electrochemical analysers. *Forensic Sci. Int.* **2008**, *178*, e29–e33. [CrossRef] [PubMed]
3. Delgado, M.K.; Shofer, F.; Wetherill, R.; Curtis, B.; Hemmons, J.; Spencer, E.; Branas, C.; Wiebe, D.J.; Kranzler, H.R. Accuracy of consumer-marketed smartphone-paired alcohol breath testing devices: A laboratory validation study. *Alcohol. Clin. Exp. Res.* **2021**, *45*, 1091–1099. [CrossRef]
4. Peris, M.; Escuder-Gilabert, L. A 21st century technique for food control: Electronic noses. *Anal. Chim. Acta* **2009**, *638*, 1–15. [CrossRef]
5. Jia, W.; Liang, G.; Wang, Y.; Wang, J. Electronic noses as a powerful tool for assessing meat quality: A mini review. *Food Anal. Methods* **2018**, *11*, 2916–2924. [CrossRef]
6. Winquist, F.; Lundström, I.; Wide, P. The combination of an electronic tongue and an electronic nose. *Sens. Actuators B Chem.* **1999**, *58*, 512–517. [CrossRef]
7. Young, R.C.; Buttner, W.J.; Linnell, B.R.; Ramesham, R. Electronic nose for space program applications. *Sens. Actuators B Chem.* **2003**, *93*, 7–16. [CrossRef]

8. Fonollosa, J.; Rodriguez-Lujan, I.; Shevade, A.V.; Homer, M.L.; Ryan, M.A.; Huerta, R. Human activity monitoring using gas sensor arrays. *Sens. Actuators B Chem.* **2014**, *199*, 398–402. [CrossRef]
9. Ryan, M.; Homer, M.; Zhou, H.; Mannatt, K.; Ryan, V.; Jackson, S. *Operation of an Electronic Nose Aboard the Space Shuttle and Directions for Research for a Second Generation Device*; SAE Technical Paper 2000-01-2512; SAE International: Warrendale, PA, USA, 2000.
10. De Vito, S.; Miglietta, M.L.; Massera, E.; Fattoruso, G.; Formisano, F.; Polichetti, T.; Salvato, M.; Alfano, B.; Esposito, E.; Di Francia, G. Electronic noses for composites surface contamination detection in aerospace industry. *Sensors* **2017**, *17*, 754. [CrossRef] [PubMed]
11. Sun, Z.H.; Liu, K.X.; Xu, X.H.; Meng, Q.H. In Odor Evaluation of Vehicle Interior Materials Based on Portable E-Nose. In Proceedings of the 2020 39th Chinese Control Conference (CCC), Shenyang, China, 27–29 July 2020; IEEE: Piscataway, NJ, USA, 2020; pp. 2998–3003.
12. Wasilewski, T.; Migon, D.; Gebicki, J.; Kamysz, W. Critical review of electronic nose and tongue instruments prospects in pharmaceutical analysis. *Anal. Chim. Acta* **2019**, *1077*, 14–29. [CrossRef]
13. Xu, J.; Liu, K.; Zhang, C. Electronic nose for volatile organic compounds analysis in rice aging. *Trends Food Sci. Technol.* **2021**, *109*, 83–93. [CrossRef]
14. Gong, J.W.; Chen, Q.F.; Lian, M.R.; Liu, N.C.; Daoust, C. Temperature feedback control for improving the stability of a semiconductor-metal-oxide (SMO) gas sensor. *IEEE Sens. J.* **2006**, *6*, 139–145.
15. Akhter, F.; Alahi, M.E.E.; Siddiquei, H.R.; Gooneratne, C.P.; Mukhopadhyay, S.C. Graphene oxide (GO) coated impedimetric gas sensor for selective detection of carbon dioxide (CO_2) with temperature and humidity compensation. *IEEE Sens. J.* **2020**, *21*, 4241–4249. [CrossRef]
16. Wang, C.; Yin, L.; Zhang, L.; Xiang, D.; Gao, R. Metal oxide gas sensors: Sensitivity and influencing factors. *Sensors* **2010**, *10*, 2088–2106. [CrossRef]
17. Mahdavi, H.; Rahbarpour, S.; Hosseini-Golgoo, S.M.; Jamaati, H. Reducing the destructive effect of ambient humidity variations on gas detection capability of a temperature modulated gas sensor by calcium chloride. *Sens. Actuators B Chem.* **2021**, *331*, 129091. [CrossRef]
18. Liang, Z.; Tian, F.; Yang, S.X.; Zhang, C.; Sun, H.; Liu, T. Study on interference suppression algorithms for electronic noses: A review. *Sensors* **2018**, *18*, 1179. [CrossRef]
19. Nebhen, J.; Meillère, S.; Masmoudi, M.; Seguin, J.L.; Barthelemy, H.; Aguir, K. Temperature compensated CMOS ring VCO for MEMS gas sensor. *Analog Integr. Circuits Signal Process.* **2013**, *76*, 225–232. [CrossRef]
20. Jiang, Y.; Zhao, Y. Design of temperature compensation system for MEMS gyroscopes based on STM32. In Proceedings of the IOP Conference Series: Materials Science and Engineering—4th Annual International Workshop on Materials Science and Engineering (IWMSE2018), Xi'an, China, 18–20 May 2018; IOP Publishing: Bristol, UK, 2018; p. 012139.
21. Zhou, G.; Zhao, Y.; Guo, F.; Xu, W. A smart high accuracy silicon piezoresistive pressure sensor temperature compensation system. *Sensors* **2014**, *14*, 12174–12190. [CrossRef]
22. Yu, X.; Lv, R.H.; Song, F.; Zheng, C.T.; Wang, Y.D. Pocket-sized nondispersive infrared methane detection device using two-parameter temperature compensation. *Spectrosc. Lett.* **2014**, *47*, 30–37. [CrossRef]
23. Xun, L. In Development of ultra-low power natural gas metering device based on pressure sensor temperature compensation method. In Proceedings of the 2015 12th IEEE International Conference on Electronic Measurement & Instruments (ICEMI), Qingdao, China, 16–18 July 2015; IEEE: Piscataway, NJ, USA, 2015; pp. 1567–1571.
24. Piao, H.; Cheng, D.; Chen, C.; Wang, Y.; Wang, P.; Pan, X. A Temperature Gradient Field Compensation Method to Improve the Accuracy of the CO_2 Carbon Isotope Sensor. *IEEE Trans. Instrum. Meas.* **2022**, *71*, 1–12. [CrossRef]
25. Zhang, C.; Wang, W.; Pan, Y.; Cheng, L.; Zhai, S.; Gao, X. A two-stage method for real-time baseline drift compensation in gas sensors. *Meas. Sci. Technol.* **2022**, *33*, 045108. [CrossRef]
26. Liu, Y.; Ma, T. Parasitic resistance-based high precision capacitive MEMS accelerometer phase shift and its usage for temperature compensation. *IEEE Sens. J.* **2017**, *18*, 629–634. [CrossRef]
27. Wang, Y.; Sun, X.; Huang, T.; Ye, L.; Song, K. Cold Starting Temperature Drift Modeling and Compensation of Micro-Accelerometer Based on High-Order Fourier Transform. *Micromachines* **2022**, *13*, 413. [CrossRef] [PubMed]
28. Xu, P.; Song, K.; Xia, X.; Chen, Y.; Wang, Q.; Wei, G. Temperature and Humidity Compensation for MOS Gas Sensor Based on Random Forests. In Proceedings of the International Conference on Intelligent Computing for Sustainable Energy and Environment (ICSEE 2017), Nanjing, China, 22–24 September 2017; pp. 135–145.
29. Hossein-Babaei, F.; Ghafarinia, V. Compensation for the drift-like terms caused by environmental fluctuations in the responses of chemoresistive gas sensors. *Sens. Actuators B Chem.* **2010**, *143*, 641–648. [CrossRef]
30. Cheng, J.; Qi, B.; Chen, D.; René, L., Jr. Modification of an RBF ANN-Based Temperature Compensation Model of Interferometric Fiber Optical Gyroscopes. *Sensors* **2015**, *15*, 11189–11207. [CrossRef] [PubMed]
31. Wang, H.; Zhang, W.; You, L.; Yuan, G.; Zhao, Y.; Jiang, Z. BACK PROPAGATION NEURAL NETWORK MODEL FOR TEMPERATURE AND HUMIDITY COMPENSATION OF A NON DISPERSIVE INFRARED METHANE SENSOR. *Instrum. Sci. Technol.* **2013**, *41*, 608–618. [CrossRef]
32. Liang, H.; Chen, H.; Lu, Y. Research on sensor error compensation of comprehensive logging unit based on machine learning. *J. Intell. Fuzzy Syst.* **2019**, *37*, 3113–3123. [CrossRef]

33. Zhu, X.; Liu, T.; Chen, J.; Cao, J.; Wang, H. One-Class Drift Compensation for an Electronic Nose. *Chemosensors* **2021**, *9*, 208. [CrossRef]
34. Dobrzyniewski, D.; Szulczynski, B.; Gebicki, J. Determination of Odor Air Quality Index (OAQII) Using Gas Sensor Matrix. *Molecules* **2022**, *27*, 4180. [CrossRef]
35. Shuba, A.; Kuchmenko, T.; Menzhulina, D. Drift Compensation of the Electronic Nose in the Development of Instruments for Out-of-Laboratory Analysis. In Proceedings of the 1st International Electronic Conference on Chemical Sensors and Analytical Chemistry (CSAC 2021), Online Conference, 1–15 July 2021.
36. Ferguson, S.A.; Zaouk, A.; Dalal, N.; Strohl, C.; Traube, E.; Strassburger, R. Driver Alcohol Detection System for Safety (DADSS)—Phase I Prototype Testing and Findings. In Proceedings of the 22nd International Technical Conference on the Enhanced Safety of Vehicles (ESV), Washington, DC, USA, 13–16 June 2011; pp. 11–0230.
37. Weng, X.H.; Luan, X.Y.; Kong, C.; Chang, Z.Y.; Li, Y.W.; Zhang, S.J.; Al-Majeed, S.; Xiao, Y.K. A Comprehensive Method for Assessing Meat Freshness Using Fusing Electronic Nose, Computer Vision, and Artificial Tactile Technologies. *J. Sens.* **2020**, *2020*, 1–14. [CrossRef]
38. Weng, X.; Sun, Y.; Xie, J.; Deng, S.; Chang, Z. Bionic Layout Optimization of Sensor Array in Electronic Nose for Oil Shale Pyrolysis Process Detection. *J. Bionic Eng.* **2021**, *18*, 441–452. [CrossRef]
39. Yan, J.; Guo, X.; Duan, S.; Jia, P.; Wang, L.; Peng, C.; Zhang, S. Electronic Nose Feature Extraction Methods: A Review. *Sensors* **2015**, *15*, 27804–27831. [CrossRef] [PubMed]
40. Zhao, X.; Li, P.; Xiao, K.; Meng, X.; Han, L.; Yu, C. Sensor Drift Compensation Based on the Improved LSTM and SVM Multi-Class Ensemble Learning Models. *Sensors* **2019**, *19*, 3844. [CrossRef] [PubMed]
41. Tian, F.; Zhang, J.; Yang, S.; Zhao, Z.; Liang, Z.; Liu, Y.; Wang, D. Suppression of Strong Background Interference on E-Nose Sensors in an Open Country Environment. *Sensors* **2016**, *16*, 233. [CrossRef] [PubMed]
42. Kalman, E.L.; LöFvendahl, A.; Winquist, F.; LundströM, I. Classification of complex gas mixtures from automotive leather using an electronic nose. *Anal. Chim. Acta* **2009**, *403*, 31–38. [CrossRef]